HHS Public Access

Author manuscript

Toxicol Appl Pharmacol. Author manuscript; available in PMC 2021 December 15.

Published in final edited form as:

Toxicol Appl Pharmacol. 2020 December 15; 409: 115301. doi:10.1016/j.taap.2020.115301.

Co-exposure to PCB126 and PFOS increases biomarkers associated with cardiovascular disease risk and liver injury in mice

Pan Deng[1,2], **Chunyan Wang**[1], **Banrida Wahlang**[3], **Travis Sexton**[4], **Andrew J. Morris**[1,4], **Bernhard Hennig**[1,5]

[1]Superfund Research Center, University of Kentucky, Lexington, KY, USA 40536

[2]Department of Pharmaceutical Sciences, College of Pharmacy, University of Kentucky, Lexington, KY, USA 40536

[3]Superfund Research Center, University of Louisville, Louisville, KY, 40202, USA

[4]Division of Cardiovascular Medicine, The Gill Heart and Vascular Institute, College of Medicine, University of Kentucky, and Lexington Veterans Affairs Medical Center, Lexington, KY, 40536

[5]Department of Animal and Food Sciences, College of Agriculture, Food and Environment, University of Kentucky, Lexington, KY, USA 40536

Abstract

Polychlorinated biphenyl (PCB)126 and perfluorooctane sulfonic acid (PFOS) are halogenated organic pollutants of high concern. Exposure to these chemicals is ubiquitous, and can lead to potential synergistic adverse effects in individuals exposed to both classes of chemicals. The present study was designed to identify interactions between PCB126 and PFOS that might promote acute changes in inflammatory pathways associated with cardiovascular disease and liver injury. Male C57BL/6 mice were exposed to vehicle, PCB126, PFOS, or a mixture of both pollutants. Plasma and liver samples were collected at 48 h after exposure. Changes in the expression of hepatic genes involved in oxidative stress, inflammation, and atherosclerosis were investigated. Plasma and liver samples was analyzed using untargeted lipidomic method. Hepatic

Corresponding author: Bernhard Hennig, PhD, Rm. 501 Wethington Health Sciences Bldg, 900 S. Limestone Street, University of Kentucky, Lexington, KY40536-0200, Phone (859) 218-1387 or 218-1343, Fax (859) 257-1811, bhennig@uky.edu.

CRediT author statement

Pan Deng: Conceptualization, Methodology, Investigation, Writing - Original Draft, Writing - Review & Editing
Chunyan Wang: Investigation, Methodology, Writing - Review & Editing,
Banrida Wahlang: Investigation, Writing - Review & Editing
Travis Sexton: Investigation, Methodology, Writing - Review & Editing,
Andrew J Morris: Resources, Funding acquisition, Writing - Review & Editing,
Bernhard Hennig: Conceptualization, Supervision, Writing - Review & Editing, Funding acquisition

Financial interests

The authors declare they have no actual or potential competing conflict of financial interest relevant to this work.

Declaration of interests

The authors declare that they have no known competing financial interests or personal relationships that could have appeared to influence the work reported in this paper.

mRNA levels for *Nqo1*, *Icam1*, and *PAI1* were significantly increased in the mixture-exposed mice. Plasma levels of PAI1, a marker of fibrosis and thrombosis, were also significantly elevated in the mixture-exposed group. Liver injury was observed only in the mixture-exposed mice. Lipidomic analysis revealed that co-exposure to the mixture enhanced hepatic lipid accumulation and elevated oxidized phospholipids levels. In summary, this study shows that acute co-exposure to PCB126 and PFOS in mice results in liver injury and increased cardiovascular disease risk.

Keywords

PFAS; PFOS; PCB126; lipid; liver; cardiovascular disease

Introduction

Per- and polyfluoroalkylated substances (PFAS) are a large class of highly fluorinated organic chemicals with a wide range of uses in industrial and consumer products. They are extremely persistent and are ubiquitously found in the environment (Anderko *et al.*, 2019). The 8-carbon perfluoroalkyls, such as perfluorooctane sulfonic acid (PFOS), have gained massive attention in the field of environmental health because of historically widespread manufacturing and use. Concerns about the health impacts from PFOS continue to grow. Epidemiology studies reported increases in serum enzymes after PFOS exposure, suggestive of liver damage (Gallo *et al.*, 2012; Zeng *et al.*, 2019). Evidence from animal studies indicated that the liver is a sensitive target of PFOS toxicity in rodents. However, given the same serum concentration, humans may be less susceptible than rodents to liver effects of perfluorinated compounds (Pizzurro *et al.*, 2019). Additionally, PFOS exposure has been associated with decreased immune responses (DeWitt *et al.*, 2019). Conflicting observations have been reported for the associations between PFOS and cardiometabolic risk factors (Sun *et al.*, 2018; Bassler *et al.*, 2019; Donat-Vargas *et al.*, 2019a; Donat-Vargas *et al.*, 2019b). Polychlorinated biphenyls (PCBs), another class of persistent organic pollutants, have been associated with numerous disorders in exposed populations. It has been well acknowledged that exposure to PCB126, a coplanar PCB congener which is “dioxin-like” in nature, is associated with increased risks for cardiovascular, liver, and metabolic diseases (Lind *et al.*, 2004; Wahlang *et al.*, 2017; Rahman *et al.*, 2019). The epidemiological association between PCBs and liver injury has been confirmed (Kumar *et al.*, 2014; Clair *et al.*, 2018). Animal experiment suggested that that monkeys are more sensitive to PCB hepatotoxicity than rodents. Liver toxic effects are similar in nature among species (Agency for Toxic Substances and Disease Registry, 2000).

Although the production of PFOS and PCB126 have been banned in many countries worldwide and human exposure levels have continued to decline, these chemicals are still detectable in many individuals. Ingestion of contaminated food and drinking water is the main route of exposure to both PFOS and PCB126 in the general population, and both chemicals are readily absorbed and poorly eliminated from humans and rodents (Yoshimura *et al.*, 1985; Ogura, 2004; Li *et al.*, 2018). The half-lives of PFOS range from days in mice (30–42 days) (Chang *et al.*, 2012) to years in humans (4.0–5.8 years) (Olsen *et al.*, 2007; Chou and Lin, 2019).The half-life of PCB126 is approximately 17 days in rodents

(Yoshimura *et al.*, 1985) and 4.5 years in humans (Ogura, 2004). Consequently, PFAS and PCBs including PFOS and PCB126 have been detected in serum in many cohorts (Lauritzen *et al.*, 2017; Petersen *et al.*, 2018; Timmermann *et al.*, 2019). However, little is known about how these two classes of environmental pollutants might interact to impact human health.

Research with individual pollutants indicated that liver is the target organ for PCB126 toxicity, and PCB126 activates the aryl hydrocarbon receptor, which results in the upregulation of detoxification enzymes. Because many of those enzymes are linked to the generation of reactive oxygen species (ROS), oxidative stress or changes in the cellular redox status are commonly associated with dioxin-like PCBs exposure (Hennig *et al.*, 2002; Ramadass *et al.*, 2003; Green *et al.*, 2008). In our previous studies, it was found that PCB126 induced oxidative stress and disrupted lipid metabolism (Wahlang *et al.*, 2017; Petriello *et al.*, 2018; Deng *et al.*, 2019). Pre-existing liver injury or a compromised liver can markedly impact PCB126-induced tissue responses which can promote vascular inflammation and liver steatosis (Wahlang *et al.*, 2017; Deng *et al.*, 2019). Similar to PCB126, PFOS can also accumulate in the liver and modulate the expression of various genes related to lipid metabolism and inflammation (Wang *et al.*, 2014; Zeng *et al.*, 2019). The current study was designed to investigate possible acute interactions between PCB126 and PFOS with a particular focus on the possibility that PFOS could modify the PCB126 toxicity to promote vascular inflammation and liver injury. Mice were exposed to either of the two pollutants, or to a mixture of PCB126 and PFOS. Expression of different genes known to be involved in PCB126 toxicity were studied in order to investigate whether the presence of PFOS would modify the patterns of toxicity. We also examined effects of exposure to these chemicals on the liver and circulating lipidome.

2. Methods

2.1 Chemicals and reagents

PCB126 was purchased from the American AccuStandard Company (purity > 99.99 %; New Haven, CT, USA). PFOS (heptadecafluorooctanesulfonic acid potassium salt, CAS 2795–39–3) was purchased from Sigma-Aldrich (purity > 98%, Saint Louis, MO, USA). Solutions of PCB126, PFOS, and a mixture of PCB126 and PFOS were dissolved in safflower oil vehicle (Dyets, Bethlehem, PA, USA) and used for animal study. The SPLASH LIPIDOMIX mass spec standard used for lipidomic assay was purchased from Avanti Polar Lipids (Alabaster, AL, USA). All solvents used in lipidomic analysis were of high-performance liquid chromatography grade.

2.2 Animal experiment

Wild type male C57BL/6 mice (8 weeks old) were purchased form Taconic (Hudson, NY, USA). The animals were allowed access to chow and water *ad libitum* and maintained at 23°C with 12/12-h light-dark cycle. The body weight was recorded before and two days after exposure. The animal protocol was approved by the University of Kentucky Institutional Animal Care and Use Committee, and a proof/certificate of approval is available upon request. The dose of PCB126 (0.5 mg/kg) was the same one used in our previous mouse studies (Wahlang *et al.*, 2017; Deng *et al.*, 2019), in which cardiometabolic

disease endpoints were analyzed, and PCB126 has been shown to induce liver injury and inflammation. The dosage of PFOS (250 mg/kg) was selected based on the total administered dose in previous animal studies (Sato *et al.*, 2009; Wang *et al.*, 2014; Wimsatt *et al.*, 2016), where PFOS has been shown to disturb lipid metabolism and 250 mg/kg is an approximate maximum tolerated dose in mouse models. The dose of PCB126 and PFOS were higher than the environmental exposure levels in humans, and the doses in the current study were chosen to maximize the potential for identifying acute adverse effects. After acclimatization for one week, all male mice were randomly divided into four groups (n = 8/group) and intragastric gavaged with a single dose of each solution: the control group (safflower oil vehicle), the PCB126-treated group (0.5 mg/kg), the PFOS-treated group (250 mg/kg), and the PCB126 plus PFOS group (mixture solution delivered at the same dosage as mice treated with individual chemicals). Two days after exposure, animals were humanely euthanized after fasting for 16 h. Blood samples were collected via cardiac puncture into an ethylenediaminetetraacetic acid-treated tube and kept on ice prior to separation of plasma at 3000 *g* centrifugation. Tissues were harvested for mRNA and lipids analyses. All biological samples were stored at −80 °C prior to analysis.

2.3 Histological studies

Sections from liver tissues were fixed in 10% neutral buffered formalin and embedded in paraffin for histological examination. Tissue sections were stained with hematoxylin-eosin (H&E) and examined by light microscopy. Reagents were obtained from Sigma-Aldrich (St. Louis, MO, USA). Photomicrographic images were captured at 20x magnification using a Nikon Eclipse Ti2 microscope (Melville, NY).

2.4 Real-time PCR

Mouse tissue samples were homogenized and total RNA was extracted using the TRIzol reagent (Thermo Fisher Scientific Inc, Waltham, MA, USA). RNA purity and quantity were assessed with the NanoDrop 2000/2000c (Thermo Fisher Scientific Inc) using the NanoDrop 2000 (Installation Version 1.6.198) software. cDNA was synthesized from total RNA using the QuantiTect Reverse Transcription Kit (Qiagen, Valencia, CA, USA). Polymerase chain reaction (PCR) was performed with the CFX96 Touch Real-Time PCR Detection System (Bio-Rad, Hercules, CA, USA) using the Taqman Fast Advanced Master Mix (Thermo Fisher Scientific Inc). Primer sequences from Taqman Gene Expression Assays (Thermo Fisher Scientific Inc) were as follows: tumor necrosis factor alpha (*Tnf*α), (Mm00443258_m1); plasminogen activator inhibitor (*PAI-1*, *Serpine 1*), (Mm00435858_m1); (NAD(P)H dehydrogenase quinone 1 (*Nqo1*), (Mm01253561_m1); E-selectin (*Sele*), (Mm00441278_m1); intercellular adhesion molecule 1 (*Icam1*), (Mm00516023_m1); and beta actin (*Actb*), (Mm02619580_g1). The hepatic levels of mRNA were normalized relative to the amount of *Actb* mRNA, and expression levels in mice administered vehicle were set at 1. Gene expression levels were calculated according to the $2^{-\Delta\Delta Ct}$ method (Livak and Schmittgen, 2001).

2.5 Measurements of cardiovascular disease and liver injury markers

The Milliplex Map Mouse CVD Magnetic Bead Panel 1 (Millipore Corp, Billerica, MA, USA) was used to measure plasma levels of PAI1, Icam1, and sE-selectin on the Luminex

Xmap MAGPIX system (Luminex Corp, Austin, TX, USA). Plasma aspartate transaminase (AST) activity and alanine transaminase (ALT) activity were measured with the Piccolo Xpress Chemistry Analyzer using Lipid Panel Plus reagent disks (CLIAwaived Inc, San Diego, CA, USA).

2.6 Lipidomic analysis of plasma and liver

Plasma and liver samples were extracted as previously reported (Deng *et al.*, 2020). Briefly, 20 μL of plasma was spiked with internal standard solution and extracted with methyl tertiary-butyl ether (MTBE) twice. The combined extract was dried under nitrogen. For liver samples, 20 mg liver tissues were homogenized and spiked with the internal standard solution. Methanol and MTBE were added and each sample was shaken for 1 h at room temperature. Phase separation was induced by adding 1.25 mL of H_2O, and the mixture was centrifuged for 10 min at 3000 *g* at 4°C. The upper lipid phase was then collected and dried under nitrogen flow. The lipid residue was dissolved in 400 μL of mixed solvent of chloroform and methanol (2:1, v/v). Lipidomic analysis was performed using an Ultimate 3000 ultra high performance liquid chromatography (UHPLC) system coupled to a Q-Exactive Orbitrap mass spectrometer (MS) equipped with a heated electrospray ion source (Thermo Scientific, CA, USA). Lipid extracts were separated on a Waters ACQUITY BEH C8 column (2.1 × 50 mm, 1.7 μm) as described in our previous report (Deng *et al.*, 2020). The mass spectrometer was operated in positive ionization mode. The full scan and fragment spectra were collected at resolutions of 70,000 and 17,500, respectively. Quality control (QC) samples prepared from pooled mouse plasma and liver extracts were used to monitor the reproducibility of the lipid extraction and mass spectrometry analyses. Data analysis and lipid identification were performed using the software LipidSearch 4.2 (Thermo Fisher Scientific). Lipids were assigned using a general database, and oxidized lipids were assigned using an Oxid GPL database in LipidSearch. The assignments were made based on both precursor and characteristic product ions. The peak areas of deuterium labeled internal standards were analyzed using Thermo Xcalibur 4.0 QuanBrowser. The peak areas for each lipid class were normalized by internal standards. The data for liver samples were further normalized to tissue weight.

2.7 Total antioxidant capacity in liver

Total antioxidant capacity (TAC) in liver was determined using a commercially available assay kit (Abcam ab65329). Liver tissue (ca. 45 mg) was homogenized in cold PBS, centrifuged at 4 °C for 10 min at 13,000 *g*, and the supernatant was used for analysis of TAC. Samples were diluted (1:4) before adding to a 96-well plate. The reaction was initiated by adding of Cu^{2+} working solution to each well, and the plate was shaken for 90 min at room temperature shielded from light. Colorimetric activity was measured by optimal density at 570 nm, and antioxidant capacity was calculated against the Trolox linear standard calibration curve.

2.8 Statistical analyses

Statistical analyses of the lipid data were performed using Metaboanalyst 4.0 web portal (www.metaboanalyst.ca). Partial least-squares discriminant analysis (PLS-DA) of lipid data was used to identify initial trends and clusters in data sets. Machine learning approaches

(heatmap, random forest) were used in the analysis of oxidized lipid data to identify oxidized phospholipids (OxPLs) that were expressed differently among groups. The heatmap was clustered by Euclidean distance measures and Ward's clustering algorithm. Random forest provides feature selection criteria on the basis of the impact of metabolites on the classification accuracy (Xia *et al.*, 2009). Statistical analyses of RT-qPCR gene expression, plasma biomarkers, and lipidomic data were performed using the GraphPad Prism version 7.04 for Windows (GraphPad Software Inc., La Jolla, CA, USA). Comparisons between groups were made by one-way ANOVA and post hoc Tukey's test considering significance at the level of $P < 0.05$. Data are expressed as mean ± SEM. To determine combined action between exposure to PCB126 and PFOS, the synergy (S) and multiplicative (V) indices were calculated as follows (Berenbaum, 1989; Ngamwong *et al.*, 2015).

Synergy index (S)

$$S = \frac{X_{PP} - X_C}{X_{PCB} + X_{PFOS} - 2 \times X_C}$$

Multiplicative index (V)

$$V = \frac{X_C \times X_{PP}}{X_{PCB} \times X_{PFOS}}$$

Where X_C is the measurements for the control mice; X_{PCB} is the corresponding value for the PCB126 exposed mice; X_{PFOS} is for PFOS exposed mice; and X_{PP} is for PCB126 and PFOS mixture exposed mice. $S = 1$ suggests no interaction between PCB126 and PFOS on hepatic genes and OxPLs, and OxPLs; $S > 1$ suggests a positive interaction (synergism); and $S < 1$ suggests a negative interaction (i.e., antagonism). For the multiplicative index (V), $V = 1$ suggests no interaction on the multiplicative scale; $V > 1$ suggests multiplicative interaction; and $V < 1$ suggests negative multiplicative interaction. Confidence intervals (CIs) were calculated using a reported method (Berenbaum, 1989; Ngamwong *et al.*, 2015).

3 Results

3.1 Effects of PFOS and/or PCB126 on body weight and hepatic genes

There were no differences in body weight among all the groups, suggesting that the dose used did not cause hypophagia (Supplementary Figure S1). PCB126 exposures in mouse models have been shown to induce hepatic toxicity through activation of oxidative stress and inflammatory pathways (Wahlang *et al.*, 2017; Petriello *et al.*, 2018). In order to examine the effects of PFOS exposure on these reported PCB126 toxicity pathways, the genes involved in PCB126-mediated inflammation (*Icam1*, *Tnfα*), redox balance (*Nrf2*, *Nqo1*), and vascular inflammation and thrombosis (*PAI1*, *Sele*) were examined. Co-exposure to PCB126 and PFOS led to minor upregulation of hepatic *Icam1* expression, and *PAI1* was significantly induced in co-exposed mice (Figure1A and B). The expression of *Nrf2* was upregulated in all three exposure groups compared with the controls, while *Nqo1* was significantly

upregulated only in the mixture-exposed group (Figure1C and D). The exposures had no effects on *Tnfa* and *Sele* (Figure1E and F). In order to understand the combined effects of PCB126 and PFOS, the *S* and *V* indices were calculated. It was found that the *S* index was 2.50 (1.21 to 3.79) and 1.27 (0.64 to 1.9) for *PAI1* and *Icam1*, respectively. The *S* index was 1.76 (0.01 to 3.51) for *Nqo1*, and the large CI was due to the variation in mixture exposed mice. These results suggest an additive synergistic effect between PCB126 and PFOS in regulating *PAI1*, *Icam1*, and *Nqo1*. The *V* index was lower than 1 for all tested genes, indicating the absence of multiplicative interaction between PCB126 and PFOS in the regulation of hepatic genes.

3.2 Effects of co-exposure on liver injury and vascular inflammation/thrombosis

Hepatic steatosis and injury were assessed by histology and measuring liver enzyme activity levels. Histological analysis of liver sections demonstrated few lipid droplets in PFOS exposed mice, while apparent microvesicular lipid accumulation was observed in mixture exposed mice when compared to other groups (arrow, Figure 2A). Additionally, inflammatory cell infiltration around the periportal area was observed in PCB126+PFOS exposed mice (arrow head), which was a sign of acute inflammation. Activity levels of plasma AST and ALT were elevated in mice co-exposed to PCB126 and PFOS when compared to other groups (Figure 2B). Analysis of plasma markers of vascular inflammation/thrombosis demonstrated that circulating levels of PAI1 protein were upregulated in co-exposed mice compared to other groups, but there were no differences in levels of Icam1 and sE-selection among groups (Figure 3).

3.3 Effects of PCB126 and/or PFOS on plasma and liver lipidome

To better understand the basis and significance for the apparent hepatic lipid accumulation observed in mice co-exposed to PCB126 and PFOS, we used high resolution mass spectrometry based lipidomics analysis. A PLS-DA was performed to identify groups of lipids that contributed to the differential effects of pollutant exposure on the mouse plasma lipidome. Compared to the control group, there were clear differences with exposures to either PFOS alone or to the mixture of PCB126 and PFOS (Supplemental Figure S2A). However, distinct separation between PFOS and the mixture was not observed, indicating that the observed effects derived from the mixture exposure were largely driven by PFOS. Further analysis of lipidomic data by one-way ANOVA revealed that there was an overall decrease in abundance of particular classes of plasma lipids after exposures to either PFOS alone or to the mixture of PCB126 and PFOS. Glycerolipids and phospholipids were the most significantly changed lipid classes (Figure 4). Specifically, the total level of monoglyceride (MG), diacylglycerol (DG), phosphatidylcholine (PC), and phosphatidylinositol (PI) were significant decreased in the PFOS and PCB126+PFOS groups compared to the control and PCB126 groups. Although the total level of ceramide (Cer) was not changed after exposures, further analysis of individual Cer species indicated that the plasma level of (*i*) Cer 22:0 was decreased in the PFOS and PCB126+PFOS group, and (*ii*) Cer 24:1 and Cer 18:2/24:1 were lower in PFOS and mixture exposed mice compared with PCB126 exposed mice (Figure 5A). On the contrary, the ratio of long-chain C16:0 ceramide to very-long-chain C24:0 ceramide (Cer C16/C24), a biomarker strongly

associated with metabolic defects (Tippetts *et al.*, 2018), was 5- to 6-fold higher with PFOS exposure and PCB126+PFOS co-exposure (Figure 5B).

PLS-DA processing of liver lipids indicated significant changes in liver lipid composition in the PFOS and PCB126+PFOS groups (Supplemental Figure S2B). The levels of DG and triacylglycerol (TG) were increased in mice exposed to either PFOS or co-exposed to PCB126+PFOS. There was no significant difference in the total level of phospholipids (Figure 6). However, detailed analyses of individual lipid species indicated that the phospholipids with saturated and mono-unsaturated fatty acid chains were increased in the PFOS and PCB126+PFOS groups. Conversely, phospholipids species with polyunsaturated double bonds, for examples C22:6, were significant decreased in the PFOS and PCB126+PFOS groups compared to the PCB126 and/or control groups (Supplemental Figure S3). Hepatic levels of cholesterol ester (ChE) were significantly increased after co-exposure to PCB126 and PFOS compared to other groups. Analysis of ChE with different fatty acyl chains indicated that ChE18:1,18:2, and 22:6 were the major contributors to the elevated hepatic ChE levels in mice co-exposed to PCB126 and PFOS (Supplemental Figure S4).

3.4 Effects of PCB126 and/or PFOS on liver oxidized phospholipids

OxPLs are generated by addition of molecular oxygen to double bonds of polyunsaturated diacyl- and alk(en)ylacyl phospholipids under conditions of oxidative stress. OxPLs are implicated in regulation of inflammation, thrombosis, angiogenesis, and other pathological processes (Bochkov *et al.*, 2010). In the present study, a total of 361 OxPLs were detected in liver samples using our untargeted LC-MS method. PLS-DA suggested significant differences in OxPLs abundance between unexposed and chemical-exposed mice, and the most pronounced changes were observed after PCB126+PFOS administration (Supplemental Figure S5). To identify major OxPLs that were different expressed between unexposed and chemical-exposed mice, ANOVA and machine learning algorithm approaches were performed. The heat map was constructed based on the top 25 OxPLs of importance (Figure 7A), which were analyzed with one way ANOVA and Fisher's LSD post-hoc analyses. Detailed information of these 25 OxPLs is summarized in Table 1. The data clearly illustrated the profound changes in lipids oxidation after exposure to either PCB126, PFOS or the mixture of PCB126+PFOS. Both Heat map and random forest analysis showed higher levels of PC(26:1+2O), PC(29:1COOH), PC(32:3+2O), and PC(34:1+2O) after mixture exposure than that of single chemicals (Figure 7A and B). The levels of these four OxPLs were further analyzed. The Synergy index (S) and Multiplicative index (V) were calculated to identify the combined effects of PCB126 and PFOS on the levels of OxPLs. The calculated S and V values are listed in Table S1. It was found that the S index was higher than 1 for all these four OxPLs, suggesting a positive interaction on the additive scale (an additive synergistic effect). Additionally, the V index was higher than 1 for PC(32:3+2O) and PC(34:1+2O), indicating a positive multiplicative interaction between PCB126 and PFOS in the induction of these two OxPLs. It should be noted that limited structural information of OxPLs could be elucidated from LC-MS analysis because the fragment spectrum was dominated by m/z 184 (the phosphocholine head group). Thus, fragments corresponding to oxidized fatty acid chains were observed as minor signals if any.

In order to gain more structural information on oxidized fatty acid chains, future studies will employ negative ionization MS detection, under which oxidized fatty acid chains will be effectively charged and detected. Derivatization and ion mobility mass spectrometry could be used to further identify isomers and determine oxidation sites (Spickett and Pitt, 2015; Deng *et al.*, 2016).

3.5 Effects of PCB126 and/or PFOS on liver TAC

TAC is the combined non-enzymatic (small molecules and proteins) antioxidant capacity, and it can be considered as a cumulative index of antioxidant status. There were no significant differences in hepatic TAC among different treatment groups (Supplemental Figure S6), suggesting that although liver lipids were oxidized after pollutant exposures, the overall hepatic antioxidant activity was maintained. This could be explained by the induction of hepatic redox genes including *Nrf2* and *Nqo1* after pollutant exposures.

4 Discussion

The current study aims at examining possible interactions between PCB126 and PFOS as determinants of vascular inflammation and dysregulation of hepatic lipid metabolism using a mouse model. On the basis of gene expression, plasma biomarkers, and lipidomics results, we demonstrated that acute co-exposure to a mixture of PCB126 and PFOS led to toxicity outcomes that were also observed after PFOS exposure. Additionally, distinct toxicity effects were observed after mixture exposure that were different from exposures to either chemical alone. For example, the PCB126+PFOS co-exposure induced apparent lipid droplet accumulation and inflammatory cell infiltration in the liver while also increasing plasma liver enzyme levels, indicative of hepatic steatosis and liver injury. Previous studies from our laboratory and others have shown that exposure to dioxin-like PCBs, such as PCB126, can induce inflammation, redox stress and atherogenic related genes (Chapados and Boucher, 2017; Wahlang *et al.*, 2017; Deng *et al.*, 2019). Assessment of transcriptional levels of those genes demonstrated that co-exposure to the mixture of PCB126 and PFOS induced expression of genes involved in vascular injury (*Icam1*), redox pathway (*Nqo1*), and thrombosis/fibrosis (*PAI1*). Moreover, consistent with hepatic gene expression, plasma levels of PAI1 were also significantly increased after co-exposure (Figure 3). Importantly, PAI1 is a marker of endothelial dysfunction and inflammation, and increased circulating levels of PAI1 have been considered as a nontraditional risk factor for cardiovascular disease (Cesari *et al.*, 2010). Collectively, the data suggest that acute co-exposure to the mixture of PCB126 and PFOS caused a distinct, enhanced toxicity pattern which was absent with individual exposures.

In order to gain more insight into potential interactions between PCB126 and PFOS in lipid metabolism, lipidomic analyses of plasma and liver samples were performed. We demonstrated that acute co-exposures to a mixture of PCB126 and PFOS led to lipid profiles that were also observed after PFOS exposure, indicating that the lipid disturbance observed in mixture exposed mice was driven by PFOS. In concordance with previously reported studies on PFOS (Haughom and Spydevold, 1992; Wan *et al.*, 2012; Lai *et al.*, 2018), both PFOS-containing exposures resulted in decreased circulating lipids (Figure 4), In contrast,

the ratio of plasma ceramide C16/C24, a biomarker for cardiometabolic disease risk and a driver of metabolic disease(Raichur *et al.*, 2014; Turpin *et al.*, 2014; Tippetts *et al.*, 2018), was increased in both the PFOS-containing groups (Figure 5B). In humans, high ceramide C16/24 ratios show a strong association with major adverse cardiac events, as well as other metabolic defects, such as insulin resistance (Laaksonen *et al.*, 2016; Lemaitre *et al.*, 2018). The induction of high ceramide C16/24 ratios with exposure to PFOS and the mixture of PCB126+PFOS warrants further investigation. The mixture exposure significantly decreased plasma levels of ChE compared with the PFOS group (Figure 4). This could be attributed to the combined effects of downregulating cholesterol export out of hepatocytes by PCB126 (Shen *et al.*, 2019), activation of PPARs by PFOS (Takacs and Abbott, 2007; Zhang *et al.*, 2014), and upregulation of fatty acid translocase by PFOS (Wan *et al.*, 2012). These metabolic events may occur simultaneously in co-exposed mice, resulting in the ChE sequestration in liver therefore decreased plasma ChE levels.

Many studies have shown that liver is the major target organ for PCB126 and PFOS bioaccumulation (Lyche *et al.*, 2004; Bogdanska *et al.*, 2011). Previous research with individual pollutants showed that exposure to PCB126 or PFOS led to accumulation of liver lipids, and thus causing steatosis (Wan *et al.*, 2012; Wang *et al.*, 2014; Wahlang *et al.*, 2017). Accordingly, in the present study, we found marked hepatic fat accumulation in mice exposed the mixture of PCB126+PFOS (Figure 2A) corresponding to increased hepatic levels of ChEs in this group (Figure 6). Notably, hepatic triglyceride was decreased upon exposure to the mixture as compared to PFOS alone (Figure 6). It was reported that PFOS induces PPARα activation in both rodents and humans (Berthiaume and Wallace, 2002; Takacs and Abbott, 2007). On the contrary, the transcript levels of PPARα were downregulated in rodent liver after PCB126 exposure (Gadupudi *et al.*, 2016). In addition to PPARα, other mechanisms exist which are responsible for the lipid dysregulation in response to PFOS and PCB126 exposures. It is not known at this time why the PCB126+PFOS mixture exposure led to decreased hepatic TG compared with PFOS. Potential mechanisms include an interaction between PCB126 and PFOS on PPARα or other transcription factors known to respond to those two chemical exposures such as pregnane X receptor (Dong *et al.*, 2016; Shi *et al.*, 2019). Understanding these mechanisms needs further investigation. It was found that the abundance of oxidized lipids was higher in the co-exposed mice (Figure 7), suggesting a contribution to the overall liver injury as evidenced by elevated plasma AST and ALT levels in these mice (Figure 2B).

Exposures to PCB126 and PFOS are known to induce oxidative stress (Qian *et al.*, 2010; Newsome *et al.*, 2014; Khansari *et al.*, 2017). Disturbed redox balance and excess reactive oxygen species (ROS) could lead to the production of OxPLs (Bochkov *et al.*, 2010). In the current study, using ANOVA and random forest analysis it was found that OxPLs were present at higher levels in mice exposed to the mixture of PCB126 and PFOS (Figure 7). Furthermore, by calculating Synergy index (S) and Multiplicative index (V), we found that PC(26:1+2O), PC(29:1COOH), PC(32:3+2O), and PC(34:1+2O) were elevated more pronounced after mixture exposure than each chemical alone. Specifically, multiplicative effects between PCB126 and PFOS were observed for PC(32:3+2O) and PC(34:1+2O). These results indicate synergistic interactions in the co-exposure group. Considerable evidence suggests that OxPLs play an important role in inflammation and cardiometabolic

diseases (Bochkov *et al.*, 2017; Boffa and Koschinsky, 2019). Notably, OxPLs are known to stimulate expression of Nrf2-dependent antioxidant genes such as *Nqo1* (Afonyushkin *et al.*, 2011), therefore, the *Nqo1* gene induction in the co-exposed group (Figure 1) may be in response to the higher OxPLs levels induced in this group. Furthermore, oxidative stress has been shown to mediate the induction of PAI1 (Swiatkowska *et al.*, 2002; Liu, 2008; Sangle and Shen, 2010), which partially explains the high hepatic gene expression and circulating levels of PAI1 in the mixture-exposed group.

Taken together, the results suggest that co-exposure to PCB126 and PFOS could promote redox stress and further enhance the production of OxPLs, which potentially led to the observed upregulation of antioxidant and atherogenic gene/protein expression profile. We hypothesize that the higher levels of OxPLs induced by the PCB126+PFOS mixture could also contribute to increased inflammation and the development of cardiometabolic disease. While this is an acute study, using a high dose of PFOS and looking at short term effects of interactions between two different pollutants classes, it is also important to consider doses relevant to human exposure and to address additional factors such as diet and longer duration of exposures, which all can modify toxicity outcomes. Future studies involving high fat diet feeding, chronic co-exposures, and a dose related with human exposure will be used to better understand the mechanistic outcomes of PCB126+PFOS mixture effects on the liver-cardiovascular axis and subsequent metabolic alterations.

5 Conclusions

The current study demonstrated the additive synergistic effects of PCB126 and PFOS on hepatic expression of redox, inflammation, and atherogenic genes, including *Nqo1*, *Icam1* and *PAI1*. Additionally, mixture exposure significant induced the circulating levels of PAI1 protein, a biomarker for cardiovascular disease risk. Furthermore, mixture exposed mice developed liver injury. Mechanistically, exposure to a mixture of PCB126 and PFOS can significantly induce a redox imbalance and lipid peroxidation. The synergistic effects of the two pollutants on PC(26:1+2O), PC(29:1COOH), PC(32:3+2O), and PC(34:1+2O) were multiplicative and/or additive, which may contribute to the activation of pathological processes. If translatable to humans, these effects might result in liver injury and increased risk of cardiovascular diseases. The work described herein provides new evidence that pollutant mixtures can induce a toxicity profile that is distinct from individual pollutant exposure, therefore underlines the importance of investigating effects of mixtures of chemicals or pollutants in risk assessment and biomonitoring experimental settings.

Supplementary Material

Refer to Web version on PubMed Central for supplementary material.

Acknowledgements

We thank Dr. Hunter N.B. Moseley (Institute for Biomedical Informatics, University of Kentucky) for helpful discussions. The current study is supported by the NIEHS/NIH grant P42ES007380 and T32ES011564, and NIGMS/NIH grant P30 GM127211 and 1S10OD021753-01A1.

Abbreviations

ALT	alanine transaminase
AST	aspartate transaminase
Cer	ceramide
ChE	cholesterol ester
DG	diacylglycerol
MG	monoglyceride
MS	mass spectrometer
MTBE	methyl tertiary-butyl ether
OxPLs	oxidised phospholipids
PC	phosphatidylcholine
PCBs	polychlorinated biphenyls
PCR	polymerase chain reaction
PFAS	per- and polyfluoroalkylated substance
PFOS	perfluorooctane sulfonic acid
PI	phosphatidylinositol
PLS-DA	partial least-squares discriminant analysis
QC	quality control
ROS	reactive oxygen species
TAC	total antioxidant activity
TG	triacylglycerol
UHPLC	ultra-high performance liquid chromatography

References

Afonyushkin T, Oskolkova OV, Binder BR, Bochkov VN, 2011 Involvement of CK2 in activation of electrophilic genes in endothelial cells by oxidized phospholipids. J. Lipid Res, 52, 98–103. [PubMed: 20934988]

Agency for Toxic Substances and Disease Registry, 2000 Toxicological Profile for Polychlorinated Biphenyls (PCBs). https://www.atsdr.cdc.gov/toxprofiles/tp17.pdf

Anderko L, Pennea E, Chalupka S, 2019 Per- and Polyfluoroalkyl Substances: An Emerging Contaminant of Concern. Annu. Rev. Nurs. Res, 38, 159–182. [PubMed: 32102961]

Bassler J, Ducatman A, Elliott M, Wen S, Wahlang B, Barnett J, Cave MC, 2019 Environmental perfluoroalkyl acid exposures are associated with liver disease characterized by apoptosis and altered serum adipocytokines. Environ. Pollut, 247, 1055–1063. [PubMed: 30823334]

Berenbaum MC, 1989 What is synergy? Pharmacol. Rev, 41, 93–141. [PubMed: 2692037]

Berthiaume J, Wallace KB, 2002 Perfluorooctanoate, perflourooctanesulfonate, and N-ethyl perfluorooctanesulfonamido ethanol; peroxisome proliferation and mitochondrial biogenesis. Toxicol. Lett, 129, 23–32. [PubMed: 11879971]

Bochkov V, Gesslbauer B, Mauerhofer C, Philippova M, Erne P, Oskolkova OV, 2017 Pleiotropic effects of oxidized phospholipids. Free Radic. Biol. Med, 111, 6–24. [PubMed: 28027924]

Bochkov VN, Oskolkova OV, Birukov KG, Levonen AL, Binder CJ, Stockl J, 2010 Generation and biological activities of oxidized phospholipids. Antioxid. Redox Signal, 12, 1009–1059. [PubMed: 19686040]

Boffa MB, Koschinsky ML, 2019 Oxidized phospholipids as a unifying theory for lipoprotein(a) and cardiovascular disease. Nat. Rev. Cardiol, 16, 305–318. [PubMed: 30675027]

Bogdanska J, Borg D, Sundstrom M, Bergstrom U, Halldin K, Abedi-Valugerdi M, Bergman A, Nelson B, Depierre J, Nobel S, 2011 Tissue distribution of (3)(5)S-labelled perfluorooctane sulfonate in adult mice after oral exposure to a low environmentally relevant dose or a high experimental dose. Toxicology, 284, 54–62. [PubMed: 21459123]

Cesari M, Pahor M, Incalzi RA, 2010 Plasminogen activator inhibitor-1 (PAI-1): a key factor linking fibrinolysis and age-related subclinical and clinical conditions. Cardiovasc. Ther, 28, e72–91. [PubMed: 20626406]

Chang SC, Noker PE, Gorman GS, Gibson SJ, Hart JA, Ehresman DJ, Butenhoff JL, 2012 Comparative pharmacokinetics of perfluorooctanesulfonate (PFOS) in rats, mice, and monkeys. Reprod. Toxicol, 33, 428–440. [PubMed: 21889587]

Chapados NA, Boucher MP, 2017 Liver metabolic disruption induced after a single exposure to PCB126 in rats. Environ. Sci. Pollut. Res. Int, 24, 1854–1861. [PubMed: 27796995]

Chou WC, Lin Z, 2019 Bayesian evaluation of a physiologically based pharmacokinetic (PBPK) model for perfluorooctane sulfonate (PFOS) to characterize the interspecies uncertainty between mice, rats, monkeys, and humans: Development and performance verification. Environ. Int, 129, 408–422. [PubMed: 31152982]

Clair HB, Pinkston CM, Rai SN, Pavuk M, Dutton ND, Brock GN, Prough RA, Falkner KC, McClain CJ, Cave MC, 2018 Liver Disease in a Residential Cohort With Elevated Polychlorinated Biphenyl Exposures. Toxicol. Sci, 164, 39–49. [PubMed: 29684222]

Deng P, Barney J, Petriello MC, Morris AJ, Wahlang B, Hennig B, 2019 Hepatic metabolomics reveals that liver injury increases PCB 126-induced oxidative stress and metabolic dysfunction. Chemosphere, 217, 140–149. [PubMed: 30415113]

Deng P, Hoffman JB, Petriello MC, Wang C-Y, Li X-S, Kraemer MP, Morris AJ, Hennig B, 2020 Dietary inulin decreases circulating ceramides by suppressing neutral sphingomyelinase expression and activity in mice. J. Lipid Res, 61, 45–53. [PubMed: 31604806]

Deng P, Zhong D, Wang X, Dai Y, Zhou L, Leng Y, Chen X, 2016 Analysis of diacylglycerols by ultra performance liquid chromatography-quadrupole time-of-flight mass spectrometry: Double bond location and isomers separation. Anal. Chim. Acta, 925, 23–33. [PubMed: 27188314]

DeWitt JC, Blossom SJ, Schaider LA, 2019 Exposure to per-fluoroalkyl and polyfluoroalkyl substances leads to immunotoxicity: epidemiological and toxicological evidence. J. Expo. Sci. Environ. Epidemiol, 29, 148–156. [PubMed: 30482935]

Donat-Vargas C, Bergdahl IA, Tornevi A, Wennberg M, Sommar J, Kiviranta H, Koponen J, Rolandsson O, Akesson A, 2019a Perfluoroalkyl substances and risk of type II diabetes: A prospective nested case-control study. Environ. Int, 123, 390–398. [PubMed: 30622063]

Donat-Vargas C, Bergdahl IA, Tornevi A, Wennberg M, Sommar J, Koponen J, Kiviranta H, Akesson A, 2019b Associations between repeated measure of plasma perfluoroalkyl substances and cardiometabolic risk factors. Environ. Int, 124, 58–65. [PubMed: 30639908]

Dong H, Curran I, Williams A, Bondy G, Yauk CL, Wade MG, 2016 Hepatic miRNA profiles and thyroid hormone homeostasis in rats exposed to dietary potassium perfluorooctanesulfonate (PFOS). Environ. Toxicol. Pharmacol, 41, 201–210. [PubMed: 26724606]

Gadupudi GS, Klaren WD, Olivier AK, Klingelhutz AJ, Robertson LW, 2016 PCB126-Induced Disruption in Gluconeogenesis and Fatty Acid Oxidation Precedes Fatty Liver in Male Rats. Toxicol. Sci, 149, 98–110. [PubMed: 26396156]

Gallo V, Leonardi G, Genser B, Lopez-Espinosa MJ, Frisbee SJ, Karlsson L, Ducatman AM, Fletcher T, 2012 Serum perfluorooctanoate (PFOA) and perfluorooctane sulfonate (PFOS) concentrations and liver function biomarkers in a population with elevated PFOA exposure. Environ. Health Perspect, 120, 655–660. [PubMed: 22289616]

Green RM, Hodges NJ, Chipman JK, O'Donovan MR, Graham M, 2008 Reactive oxygen species from the uncoupling of human cytochrome P450 1B1 may contribute to the carcinogenicity of dioxin-like polychlorinated biphenyls. Mutagenesis, 23, 457–463. [PubMed: 18583386]

Haughom B, Spydevold O, 1992 The mechanism underlying the hypolipemic effect of perfluorooctanoic acid (PFOA), perfluorooctane sulphonic acid (PFOSA) and clofibric acid. Biochim. Biophys. Acta, 1128, 65–72. [PubMed: 1327145]

Hennig B, Hammock BD, Slim R, Toborek M, Saraswathi V, Robertson LW, 2002 PCB-induced oxidative stress in endothelial cells: modulation by nutrients. Int. J. Hyg. Environ. Health, 205, 95–102. [PubMed: 12018021]

Khansari MR, Yousefsani BS, Kobarfard F, Faizi M, Pourahmad J, 2017 In vitro toxicity of perfluorooctane sulfonate on rat liver hepatocytes: probability of distructive binding to CYP 2E1 and involvement of cellular proteolysis. Environ. Sci. Pollut. Res. Int, 24, 23382–23388. [PubMed: 28842823]

Kumar J, Lind L, Salihovic S, van Bavel B, Ingelsson E, Lind PM, 2014 Persistent organic pollutants and liver dysfunction biomarkers in a population-based human sample of men and women. Environ. Res, 134, 251–256. [PubMed: 25173059]

Laaksonen R, Ekroos K, Sysi-Aho M, Hilvo M, Vihervaara T, Kauhanen D, Suoniemi M, Hurme R, Marz W, Scharnagl H, Stojakovic T, Vlachopoulou E, Lokki ML, Nieminen MS, Klingenberg R, Matter CM, Hornemann T, Juni P, Rodondi N, Raber L, Windecker S, Gencer B, Pedersen ER, Tell GS, Nygard O, Mach F, Sinisalo J, Luscher TF, 2016 Plasma ceramides predict cardiovascular death in patients with stable coronary artery disease and acute coronary syndromes beyond LDL-cholesterol. Eur. Heart J, 37, 1967–1976. [PubMed: 27125947]

Lai KP, Ng AH, Wan HT, Wong AY, Leung CC, Li R, Wong CK, 2018 Dietary Exposure to the Environmental Chemical, PFOS on the Diversity of Gut Microbiota, Associated With the Development of Metabolic Syndrome. Front. Microbiol, 9, 2552. [PubMed: 30405595]

Lauritzen HB, Larose TL, Oien T, Sandanger TM, Odland JO, van de Bor M, Jacobsen GW, 2017 Maternal serum levels of perfluoroalkyl substances and organochlorines and indices of fetal growth: a Scandinavian case-cohort study. Pediatr. Res, 81, 33–42. [PubMed: 27656770]

Lemaitre RN, Yu C, Hoofnagle A, Hari N, Jensen PN, Fretts AM, Umans JG, Howard BV, Sitlani CM, Siscovick DS, King IB, Sotoodehnia N, McKnight B, 2018 Circulating Sphingolipids, Insulin, HOMA-IR, and HOMA-B: The Strong Heart Family Study. Diabetes, 67, 1663–1672. [PubMed: 29588286]

Li Y, Fletcher T, Mucs D, Scott K, Lindh CH, Tallving P, Jakobsson K, 2018 Half-lives of PFOS, PFHxS and PFOA after end of exposure to contaminated drinking water. Occup. Environ. Med, 75, 46–51. [PubMed: 29133598]

Lind PM, Orberg J, Edlund UB, Sjoblom L, Lind L, 2004 The dioxin-like pollutant PCB 126 (3,3',4,4',5-pentachlorobiphenyl) affects risk factors for cardiovascular disease in female rats. Toxicol. Lett, 150, 293–299. [PubMed: 15110081]

Liu RM, 2008 Oxidative stress, plasminogen activator inhibitor 1, and lung fibrosis. Antioxid. Redox Signal, 10, 303–319. [PubMed: 17979497]

Livak KJ, Schmittgen TD, 2001 Analysis of relative gene expression data using real-time quantitative PCR and the 2(-Delta Delta C(T)) Method. Methods, 25, 402–408. [PubMed: 11846609]

Lyche JL, Skaare JU, Larsen HJ, Ropstad E, 2004 Levels of PCB 126 and PCB 153 in plasma and tissues in goats exposed during gestation and lactation. Chemosphere, 55, 621–629. [PubMed: 15006515]

Newsome BJ, Petriello MC, Han SG, Murphy MO, Eske KE, Sunkara M, Morris AJ, Hennig B, 2014 Green tea diet decreases PCB 126-induced oxidative stress in mice by up-regulating antioxidant enzymes. J. Nutr. Biochem, 25, 126–135. [PubMed: 24378064]

Ngamwong Y, Tangamornsuksan W, Lohitnavy O, Chaiyakunapruk N, Scholfield CN, Reisfeld B, Lohitnavy M, 2015 Additive Synergism between Asbestos and Smoking in Lung Cancer Risk: A Systematic Review and Meta-Analysis. PLoS One, 10, e0135798. [PubMed: 26274395]

Ogura I, 2004 Half-life of each dioxin and PCB congener in the human body. Organohalogen Compd, 66, 3329–3337.

Olsen GW, Burris JM, Ehresman DJ, Froehlich JW, Seacat AM, Butenhoff JL, Zobel LR, 2007 Half-life of serum elimination of perfluorooctanesulfonate,perfluorohexanesulfonate, and perfluorooctanoate in retired fluorochemical production workers. Environ. Health Perspect, 115, 1298–1305. [PubMed: 17805419]

Petersen MS, Halling J, Jorgensen N, Nielsen F, Grandjean P, Jensen TK, Weihe P, 2018 Reproductive Function in a Population of Young Faroese Men with Elevated Exposure to Polychlorinated Biphenyls (PCBs) and Perfluorinated Alkylate Substances (PFAS). Int. J. Environ. Res. Public Health, 15.

Petriello MC, Brandon JA, Hoffman J, Wang C, Tripathi H, Abdel-Latif A, Ye X, Li X, Yang L, Lee E, Soman S, Barney J, Wahlang B, Hennig B, Morris AJ, 2018 Dioxin-like PCB 126 Increases Systemic Inflammation and Accelerates Atherosclerosis in Lean LDL Receptor-Deficient Mice. Toxicol. Sci, 162, 548–558. [PubMed: 29216392]

Pizzurro DM, Seeley M, Kerper LE, Beck BD, 2019 Interspecies differences in perfluoroalkyl substances (PFAS) toxicokinetics and application to health-based criteria. Regul. Toxicol. Pharmacol, 106, 239–250. [PubMed: 31078680]

Qian Y, Ducatman A, Ward R, Leonard S, Bukowski V, Lan Guo N, Shi X, Vallyathan V, Castranova V, 2010 Perfluorooctane sulfonate (PFOS) induces reactive oxygen species (ROS) production in human microvascular endothelial cells: role in endothelial permeability. J. Toxicol. Environ. Health A, 73, 819–836. [PubMed: 20391123]

Rahman ML, Zhang C, Smarr MM, Lee S, Honda M, Kannan K, Tekola-Ayele F, Buck Louis GM, 2019 Persistent organic pollutants and gestational diabetes: A multi-center prospective cohort study of healthy US women. Environ. Int, 124, 249–258. [PubMed: 30660025]

Raichur S, Wang ST, Chan PW, Li Y, Ching J, Chaurasia B, Dogra S, Ohman MK, Takeda K, Sugii S, Pewzner-Jung Y, Futerman AH, Summers SA, 2014 CerS2 haploinsufficiency inhibits beta-oxidation and confers susceptibility to diet-induced steatohepatitis and insulin resistance. Cell Metab, 20, 687–695. [PubMed: 25295789]

Ramadass P, Meerarani P, Toborek M, Robertson LW, Hennig B, 2003 Dietary flavonoids modulate PCB-induced oxidative stress, CYP1A1 induction, and AhR-DNA binding activity in vascular endothelial cells. Toxicol. Sci, 76, 212–219. [PubMed: 12970578]

Sangle GV, Shen GX, 2010 Signaling mechanisms for oxidized LDL-induced oxidative stress and the upregulation of plasminogen activator inhibitor-I in vascular cells. Clin. Lipidol, 5, 221–232.

Sato I, Kawamoto K, Nishikawa Y, Tsuda S, Yoshida M, Yaegashi K, Saito N, Liu W, Jin Y, 2009 Neurotoxicity of perfluorooctane sulfonate (PFOS) in rats and mice after single oral exposure. J. Toxicol. Sci, 34, 569–574. [PubMed: 19797866]

Shen X, Chen Y, Zhang J, Yan X, Liu W, Guo Y, Shan Q, Liu S, 2019 Low-dose PCB126 compromises circadian rhythms associated with disordered glucose and lipid metabolism in mice. Environ. Int, 128, 146–157. [PubMed: 31055201]

Shi H, Jan J, Hardesty JE, Falkner KC, Prough RA, Balamurugan AN, Mokshagundam SP, Chari ST, Cave MC, 2019 Polychlorinated biphenyl exposures differentially regulate hepatic metabolism and pancreatic function: Implications for nonalcoholic steatohepatitis and diabetes. Toxicol. Appl. Pharmacol, 363, 22–33. [PubMed: 30312631]

Spickett CM, Pitt AR, 2015 Oxidative lipidomics coming of age: advances in analysis of oxidized phospholipids in physiology and pathology. Antioxid. Redox Signal, 22, 1646–1666. [PubMed: 25694038]

Sun Q, Zong G, Valvi D, Nielsen F, Coull B, Grandjean P, 2018 Plasma Concentrations of Perfluoroalkyl Substances and Risk of Type 2 Diabetes: A Prospective Investigation among U.S. Women. Environ. Health Perspect, 126, 037001. [PubMed: 29498927]

Swiatkowska M, Szemraj J, Al-Nedawi KN, Pawlowska Z, 2002 Reactive oxygen species upregulate expression of PAI-1 in endothelial cells. Cell Mol. Biol. Lett, 7, 1065–1071. [PubMed: 12511973]

Takacs ML, Abbott BD, 2007 Activation of mouse and human peroxisome proliferator-activated receptors (alpha, beta/delta, gamma) by perfluorooctanoic acid and perfluorooctane sulfonate. Toxicol. Sci, 95, 108–117. [PubMed: 17047030]

Timmermann CAG, Pedersen HS, Budtz-Jorgensen E, Bjerregaard P, Oulhote Y, Weihe P, Nielsen F, Grandjean P, 2019 Environmental chemical exposures among Greenlandic children in relation to diet and residence. Int J Circumpolar Health, 78, 1642090. [PubMed: 31339476]

Tippetts TS, Holland WL, Summers SA, 2018 The ceramide ratio: a predictor of cardiometabolic risk. J. Lipid Res, 59, 1549–1550. [PubMed: 29987126]

Turpin SM, Nicholls HT, Willmes DM, Mourier A, Brodesser S, Wunderlich CM, Mauer J, Xu E, Hammerschmidt P, Bronneke HS, Trifunovic A, LoSasso G, Wunderlich FT, Kornfeld JW, Bluher M, Kronke M, Bruning JC, 2014 Obesity-induced CerS6-dependent C16:0 ceramide production promotes weight gain and glucose intolerance. Cell Metab, 20, 678–686. [PubMed: 25295788]

Wahlang B, Barney J, Thompson B, Wang C, Hamad OM, Hoffman JB, Petriello MC, Morris AJ, Hennig B, 2017 Editor's Highlight: PCB126 Exposure Increases Risk for Peripheral Vascular Diseases in a Liver Injury Mouse Model. Toxicol. Sci, 160, 256–267. [PubMed: 28973532]

Wan HT, Zhao YG, Wei X, Hui KY, Giesy JP, Wong CK, 2012 PFOS-induced hepatic steatosis, the mechanistic actions on beta-oxidation and lipid transport. Biochim. Biophys. Acta, 1820, 1092–1101. [PubMed: 22484034]

Wang L, Wang Y, Liang Y, Li J, Liu Y, Zhang J, Zhang A, Fu J, Jiang G, 2014 PFOS induced lipid metabolism disturbances in BALB/c mice through inhibition of low density lipoproteins excretion. Sci Rep, 4, 4582. [PubMed: 24694979]

Wimsatt J, Villers M, Thomas L, Kamarec S, Montgomery C, Yeung LW, Hu Y, Innes K, 2016 Oral perfluorooctane sulfonate (PFOS) lessens tumor development in the APC(min) mouse model of spontaneous familial adenomatous polyposis. BMC Cancer, 16, 942. [PubMed: 27927180]

Xia J, Psychogios N, Young N, Wishart DS, 2009 MetaboAnalyst: a web server for metabolomic data analysis and interpretation. Nucleic Acids Res, 37, W652–660. [PubMed: 19429898]

Yoshimura H, Yoshihara S, Koga N, Nagata K, Wada I, Kuroki J, Hokama Y, 1985 Inductive effect on hepatic enzymes and toxicity of congeners of PCBs and PCDFs. Environ. Health Perspect, 59, 113–119. [PubMed: 3921354]

Zeng Z, Song B, Xiao R, Zeng G, Gong J, Chen M, Xu P, Zhang P, Shen M, Yi H, 2019 Assessing the human health risks of perfluorooctane sulfonate by in vivo and in vitro studies. Environ. Int, 126, 598–610. [PubMed: 30856447]

Zhang L, Ren XM, Wan B, Guo LH, 2014 Structure-dependent binding and activation of perfluorinated compounds on human peroxisome proliferator-activated receptor gamma. Toxicol. Appl. Pharmacol, 279, 275–283. [PubMed: 24998974]

- Toxicity pattern for the PCB126 and PFOS mixture was distinct from single chemicals.
- Cardiovascular disease biomarker PAI1 was upregulated after mixture exposure.
- Mixture exposure induced higher OxPLs production in liver.
- Mixture exposure led to liver injury which was related with lipid dysregulation.

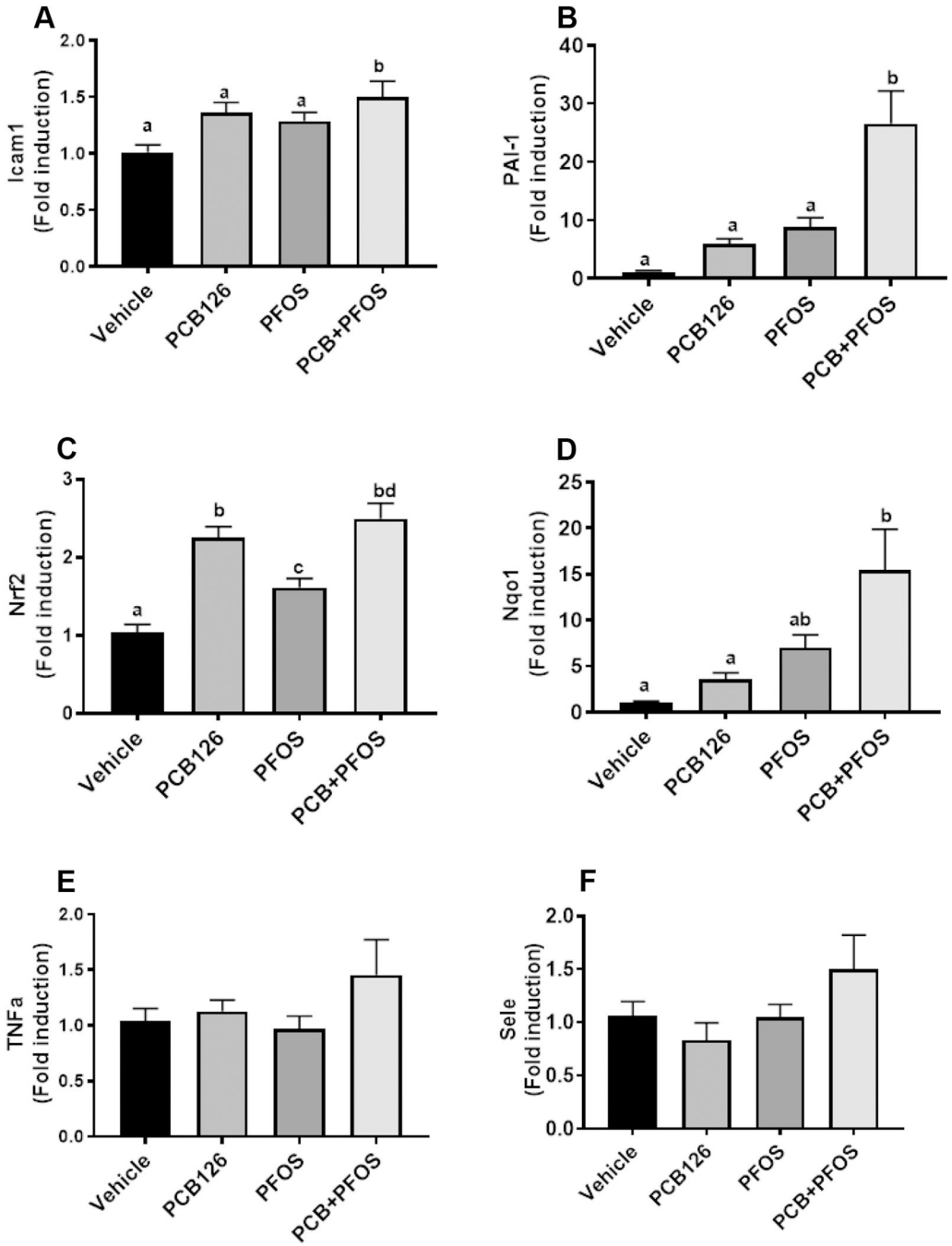

Figure 1. Hepatic gene expression in mice exposed to PCB126 (0.5 mg/kg), PFOS (250mg/kg), and a mixture of PCB126 (0.5 mg/kg) and PFOS (250mg/kg).

Hepatic expression of inflammation, atherogenic, and redox genes, including *Icam1* (A), *PAI1* (B), *Nrf2* (C), *Nqo1* (D), *Tnfα* (E), and *Sele* (F). Bars represent mean ± SEM of eight animals in each group. Different subscript letters (a, b, c) indicate statistical significance ($p<0.05$) by one-way ANOVA and post hoc Tukey's test.

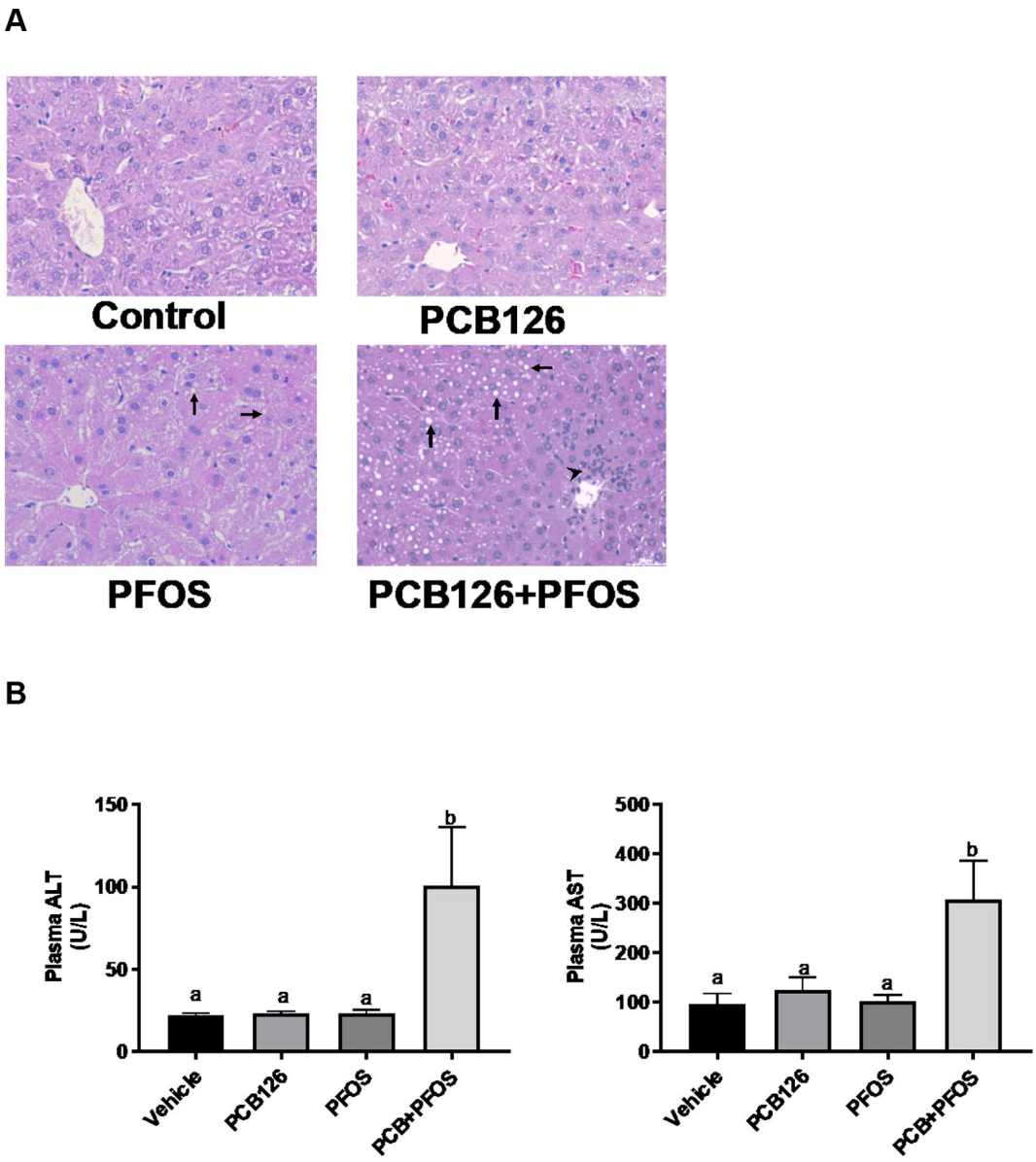

Figure 2. Effects of PCB126 (0.5 mg/kg), PFOS (250 mg/kg), and PCB126+PFOS (0.5 mg/kg+250 mg/kg) mixture exposure on liver injury.

(A) H&E staining of hepatic sections established the apparent lipid accumulation (arrow) and inflammatory cell infiltration around the periportal area (arrow head) in the mixture exposed group. (B) Elevated plasma ALT and AST levels were observed in the mixture exposed group. Bars represent mean ± SEM of eight animals in each group. Different subscript letters (a, b, c) indicate statistical significance ($p<0.05$) by one-way ANOVA and post hoc Tukey's test.

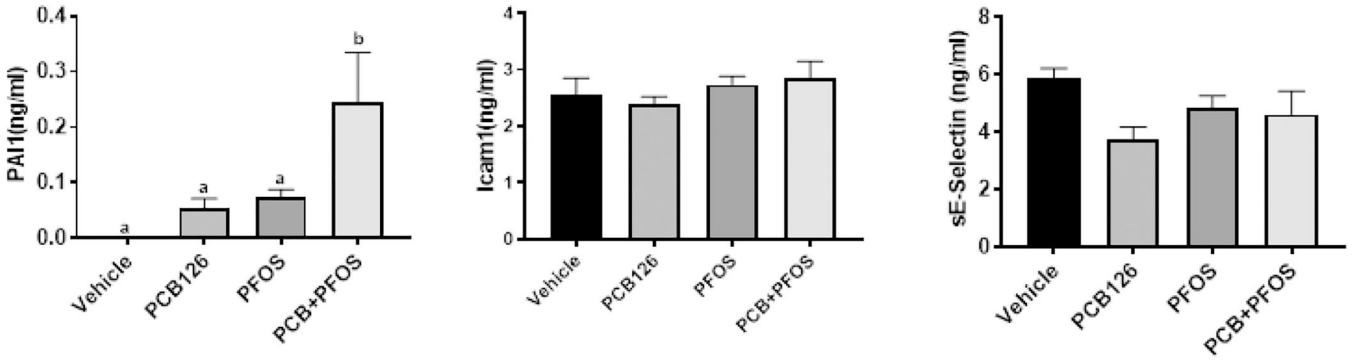

Figure 3. Effects of PCB126 (0.5 mg/kg), PFOS (250 mg/kg), and PCB126+PFOS (0.5 mg/kg+250 mg/kg) mixture exposure on markers of cardiovascular disease.

Plasma levels of PAI1, Icam1, and sE-selectin were measured using the MAGPIX system. Bars represent mean ± SEM of eight animals in each group. Different subscript letters (a, b) indicate statistical significance ($p<0.05$) by one-way ANOVA and post hoc Tukey's test.

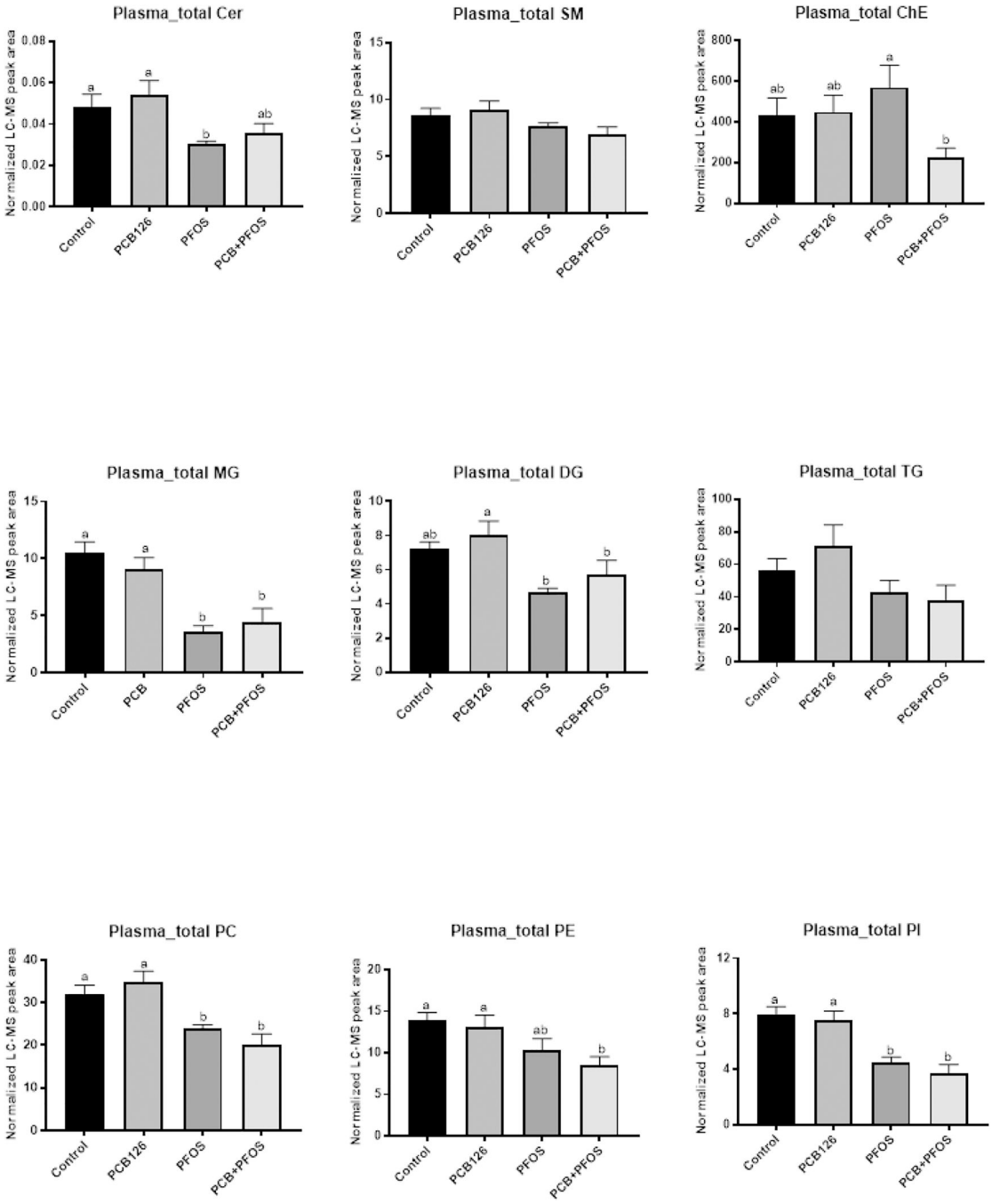

Figure 4. Effects of PCB126 (0.5 mg/kg), PFOS (250 mg/kg), and PCB126+PFOS (0.5 mg/kg+250 mg/kg) mixture exposure on plasma lipid levels.

Lipids including cholesterol ester (ChE), sphingolipids (Cer, SM), neutral lipids (MG, DG, TG), and phospholipids (PC, PE, PI) were analyzed using UHPLC-Q Exactive mass spectrometer. The normalized peak areas of lipid species in each lipid class were summarized. Bars represent mean ± SEM of eight animals in each group. Different subscript letters (a, b) indicate statistical significance ($p<0.05$) by one-way ANOVA and post hoc Tukey's test.

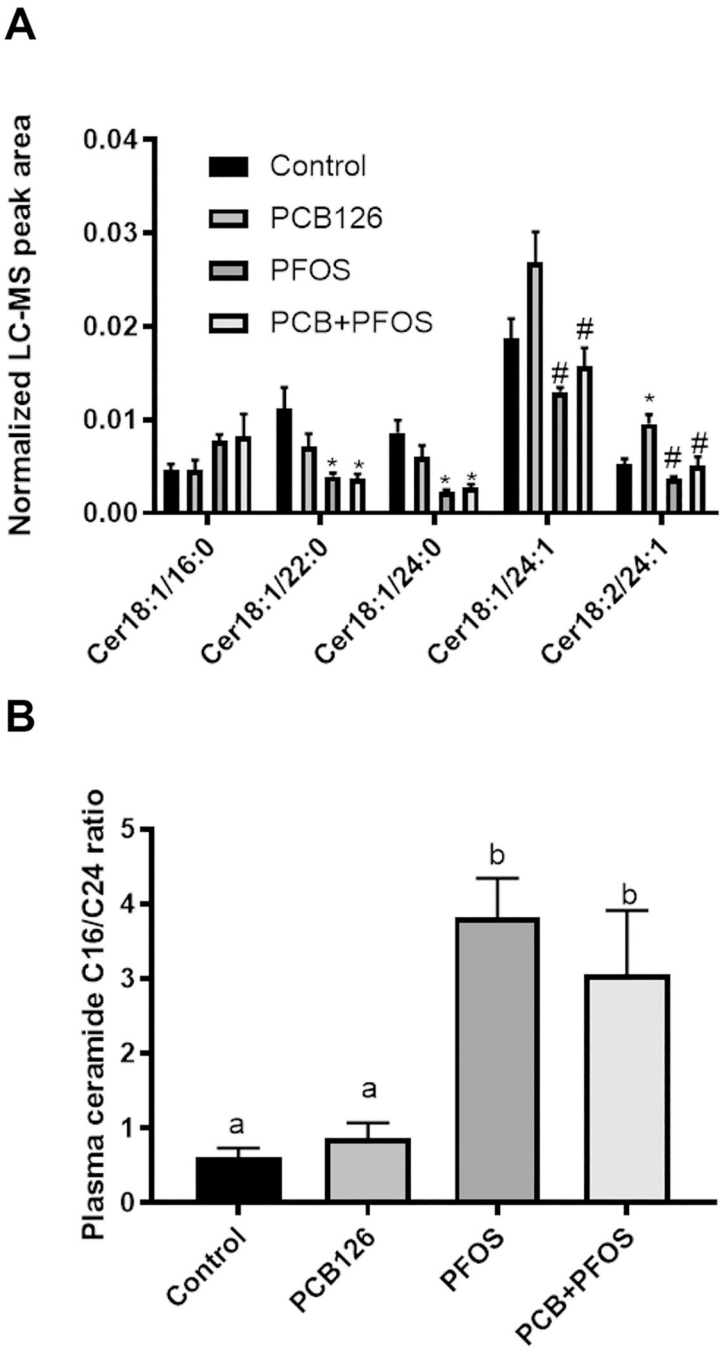

Figure 5. Effects of PCB126 (0.5 mg/kg), PFOS (250 mg/kg), and PCB126+PFOS (0.5 mg/kg+250 mg/kg) mixture exposure on plasma levels of ceramides and the ratio of ceramide C16/C24.

Ceramides were analyzed using UHPLC-Q Exactive mass spectrometer. Bars represent mean ± SEM of eight animals in each group. * $p < 0.05$ versus control mice, # $p < 0.05$ versus PCB126 exposed mice. Different subscript letters (a, b) indicate statistical significance ($p<0.05$) by one-way ANOVA and post hoc Tukey's test.

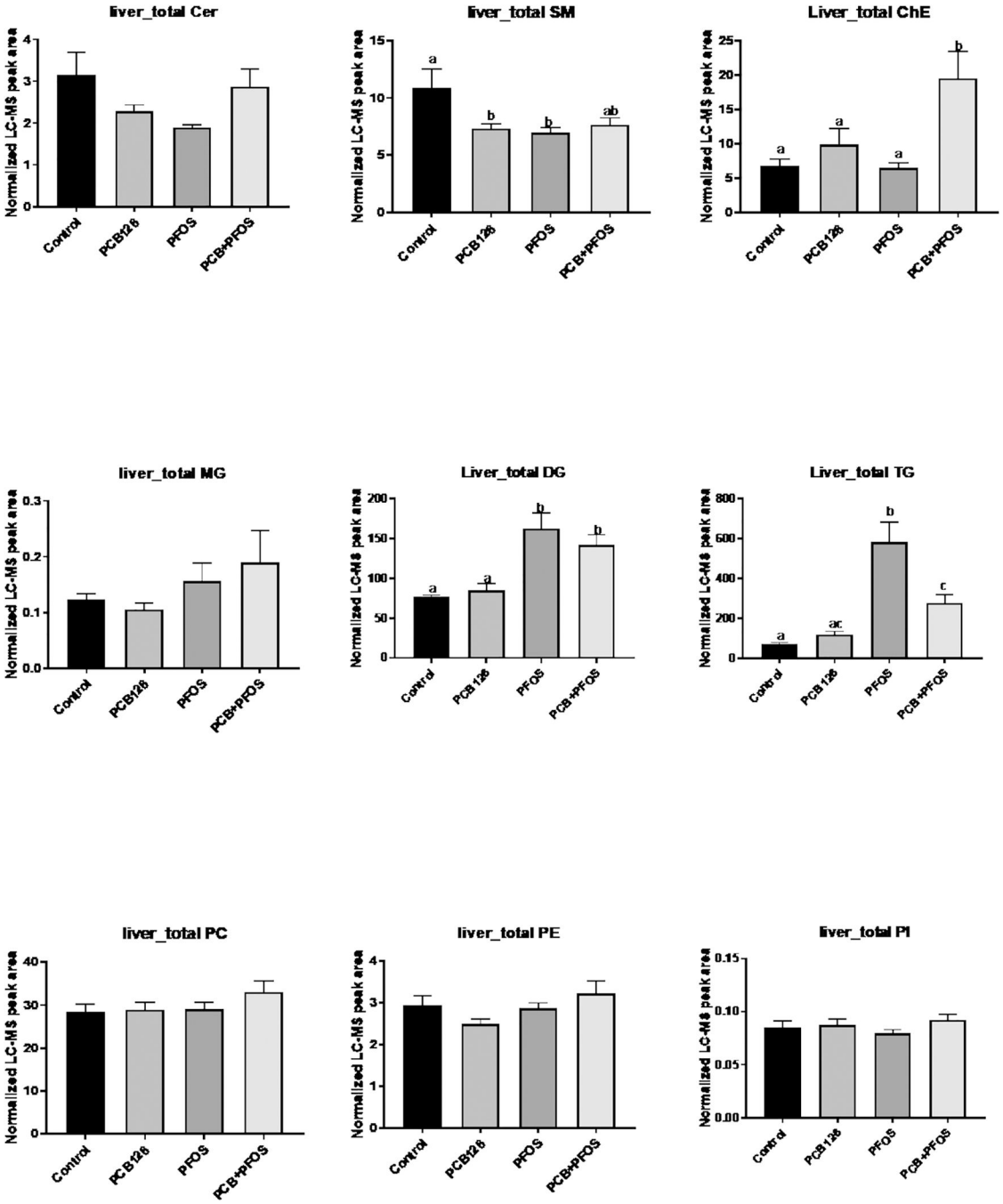

Figure 6. Effects of PCB126 (0.5 mg/kg), PFOS (250 mg/kg), and PCB126+PFOS (0.5 mg/kg+250 mg/kg) mixture exposure on liver lipid levels.

Lipids including cholesterol ester (ChE), sphingolipids (Cer, SM), neutral lipids (MG, DG, TG), and phospholipids (PC, PE, PI) were analyzed using UHPLC-Q Exactive mass spectrometer. The normalized peak areas of lipid species in each lipid class were summarized. Bars represent mean ± SEM of eight animals in each group. Different subscript letters (a, b, c) indicate statistical significance ($p<0.05$) by one-way ANOVA and post hoc Tukey's test.

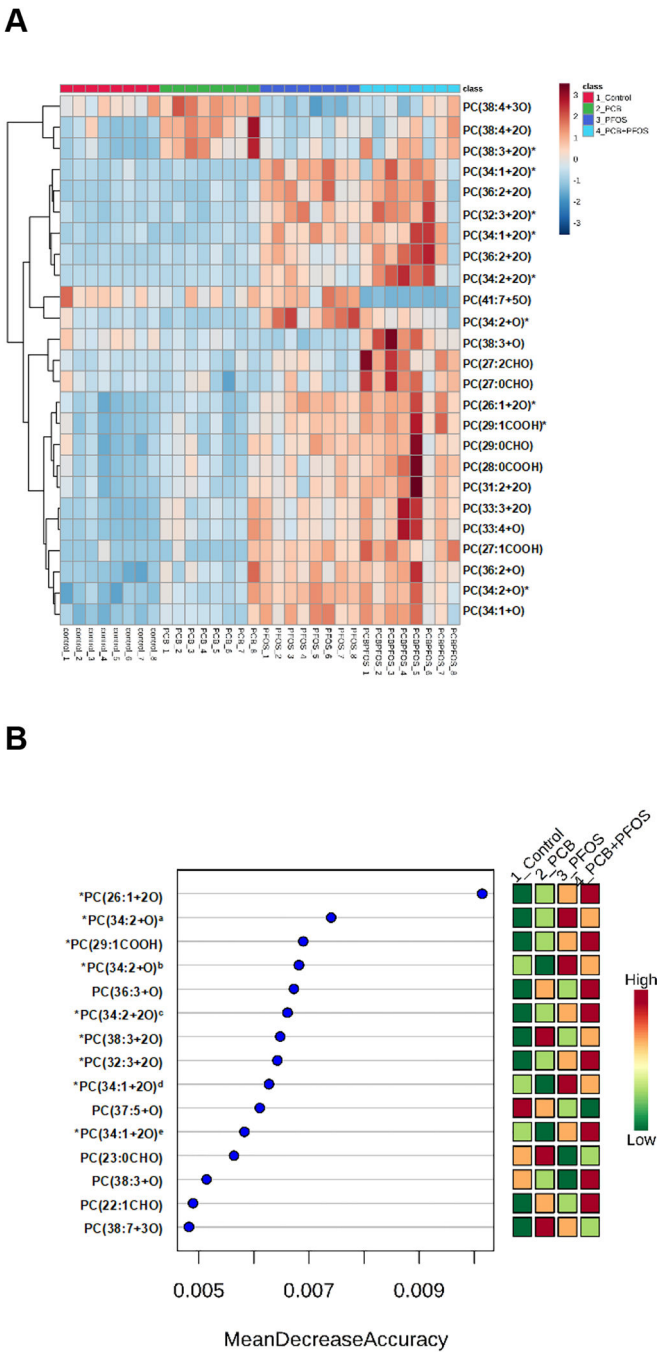

Figure 7. Effects of PCB126 (0.5 mg/kg), PFOS (250 mg/kg), and PCB126+PFOS (0.5 mg/kg+250 mg/kg) mixture exposure on liver OxPLs profiles.

OxPLs were analyzed using UHPLC-Q Exactive mass spectrometer. (A) Heat map showing the top 25 OxPLs that were differentially expressed in different groups identified using ANOVA. Each column corresponds to the OxPLs from an individual mouse, and each row corresponds to a given OxPLs. (B) Variable-importance plot of the top OxPLs identified by random forest analysis. The mean accuracy value decrease is a measure of how much predictive power is lost if a given metabolite is removed or permuted in the random forest algorithm; thus, the more important a metabolite is to classifying samples into time point

categories, the further to the right its point is on the graph. *: OxPLs identified by both ANOVA and random forest analysis. [a]: PC(34:2+O) with the retention time at 7.49 min, [b]: PC(34:2+O) with the retention time at 8.33 min, [c]: PC(34:2+2O) with the retention time at 8.77 min, [d]: PC(34:1+2O) with the retention time at 6.47 min, [e]: PC(34:1+2O) with the retention time at 8.59 min. See also Table 1 for detailed information on OxPLs.

Table 1.

Detailed information of the top 25 OxPLs that differentially expressed in liver samples from control, PCB126, PFOS, and PCB126+PFOS mixture exposed mice.

Species	Ion Formula	Rt (min)	*m/z* Observed ([M+H]+)	Δppm
PC(38:4+3O)	C46 H85 O11 N1 P1	9.23	858.5855	0.002
PC(38:4+2O)	C46 H85 O10 N1 P1	8.55	842.5900	0.682
PC(38:3+2O)	C46 H87 O10 N1 P1	8.13	844.6062	0.004
PC(34:1+2O)	C42 H83 O10 N1 P1	6.47	792.5749	0.004
PC(36:2+2O)	C44 H85 O10 N1 P1	8.38	818.5906	0.004
PC(32:3+2O)	C40 H75 O10 N1 P1	8.47	760.5123	0.005
PC(34:1+2O)	C42 H83 O10 N1 P1	8.59	792.5749	0.004
PC(36:2+2O)	C44 H85 O10 N1 P1	8.78	818.5906	0.004
PC(34:2+2O)	C42 H81 O10 N1 P1	8.77	790.5593	0.004
PC(41:7+5O)	C49 H85 O13 N1 P1	8.89	926.5753	0.002
PC(34:2+O)	C42 H81 O9 N1 P1	8.33	774.5645	0.202
PC(38:3+O)	C46 H87 O9 N1 P1	9.70	828.6101	1.449
PC(27:2CHO)	C35 H65 O9 N1 P1	2.78	674.4396	0.621
PC(27:0CHO)	C35 H69 O9 N1 P1	5.16	678.4703	0.211
PC(26:1+2O)	C34 H67 O10 N1 P1	4.35	680.4499	0.256
PC(29:1COOH)	C37 H71 O10 N1 P1	5.42	720.4806	0.599
PC(29:0CHO)	C37 H73 O9 N1 P1	5.51	706.5018	0.002
PC(28:0COOH)	C36 H71 O10 N1 P1	5.70	708.4813	0.419
PC(31:2+2O)	C39 H75 O10 N1 P1	6.46	748.5135	1.556
PC(33:3+2O)	C41 H77 O10 N1 P1	7.34	774.5280	0.004
PC(33:4+O)	C41 H75 O9 N1 P1	7.33	756.5174	0.002
PC(27:1COOH)	C35 H67 O10 N1 P1	3.31	692.4497	0.005
PC(36:2+O)	C44 H85 O9 N1 P1	8.28	802.5944	1.529
PC(34:2+O)	C42 H81 O9 N1 P1	7.49	774.5634	1.228
PC(34:1+O)	C42 H83 O9 N1 P1	7.40	776.5800	0.002